PSFC/JA-08-11

Spontaneous Core Toroidal Rotation in Alcator C-Mod L-Mode, H-Mode and ITB Plasmas.

Rice, J.E.; Ince-Cushman, A.C.; Reinke, M.L.; Podpaly, Y.;

Greenwald, M.J.; LaBombard, B.S.; Marmar, E.S.

Plasma Science and Fusion Center
Massachusetts Institute of Technology
Cambridge MA 02139 USA

M.I.T. Plasma Science and Fusion Center - Cambridge, Massachusetts 02139

This work was supported by the U.S. Department of Energy, Grant No. DE-FC02-99ER54512.

Submitted for publication to *Plasma Physics Control Fusion.*

Spontaneous Core Toroidal Rotation in Alcator C-Mod L-mode, H-mode and ITB Plasmas

J.E. Rice, A.C. Ince-Cushman, M.L. Reinke, Y. Podpaly,
M.J. Greenwald, B. LaBombard and E.S. Marmar
Plasma Science and Fusion Center, MIT, Cambridge, MA 02139-4307

Abstract

Spontaneous toroidal rotation, self-generated in the absence of external momentum input, exhibits a rich phenomenology. In L-mode plasmas, the rotation varies in a complicated fashion with electron density, magnetic configuration and plasma current, and is predominantly in the counter-current direction. The rotation depends sensitively on the balance between upper and lower null, and plays a crucial role in the H-mode power threshold. Rotation inversion between the counter- and co-current direction has been observed following small changes in the electron density and plasma current, with very distinct thresholds. In contrast, the intrinsic rotation in H-mode plasmas has a relatively simple parameter dependence, with the rotation velocity proportional to the plasma stored energy normalized to the plasma current, and is nearly always directed co-current. In plasmas with internal transport barriers, formed either with off-axis ICRF heating or LHCD, the rotation velocity inside of the ITB foot increments in the counter-current direction as the barrier evolves.

I. Introduction

In tokamak discharges, rotation and velocity shear play important roles in the transition to high confinement mode (H-mode) [1, 2, 3, 4, 5], in the formation of internal transport barriers (ITBs) [6, 7] and in suppression of resistive wall modes (RWMs) [8, 9]. On most devices, the toroidal rotation is driven externally by neutral beam injection. In future reactors like ITER, beam injection may be of limited utility and other approaches for generation and control of rotation need to be investigated. One possible solution is to take advantage of the intrinsic (spontaneous, self-generated in the absence of external momentum input) rotation widely observed under a variety of operating conditions [10]. A comparison of spontaneous rotation in H-mode plasmas from several devices leads to a relatively simple scaling, with the observed Mach number proportion to the normalized pressure [10]. This scaling obtains over a wide range of operational parameter space, and for H-modes produced by many different techniques (ICRF heating, Ohmic heating, electron cyclotron heating), indicating the universality of the phenomenon. Extrapolation to ITER plasmas suggests RWMs may be suppressed without external momentum input. In order to take full advantage of spontaneous rotation, including velocity profile control, a fundamental understanding of the underlying mechanism(s) is desireable. A complete understanding of spontaneous rotation must also address L-mode discharges, in which the rotation is comparatively much more complicated in the parameter dependences [11, 12, 13, 14, 15, 16, 17], since the rotation in L-mode is known to play an important role in the H-mode power threshold [11, 12, 18, 16].

Alcator C-Mod [19] plasmas have been formed in a variety of magnetic topologies: lower single null (LSN), double null (DN), upper single null (USN) and inner wall limited. H-mode can be accessed through auxiliary heating produced with 4 MW of ion cyclotron range of frequencies (ICRF) heating power at 80 MHz, which is coupled to the plasma by 2 two-strap antennas. An additional 4 MW of ICRF power are available with frequency between 50 and 80 MHz from a variable phase four-strap antenna. For the plasmas described here, the hydrogen minority heating was with $0 - \pi$ phasing, and there was no momentum input. Lower hybrid current drive (LHCD) power is also available, injected by a 96 wave guide, 2-way launcher capable of delivering up to 1.2 MW at 4.6 GHz, with an $n_{||}$ in the range of 1.5-3 [20]. Core toroidal rotation measurements are provided from the Doppler shifts of argon and molybdenum x-ray lines recorded by an array of von Hamos type x-ray crystal spectrometers [21] and an imaging Johann x-ray spectrometer system [22].

An outline of the paper is as follows: in II, rotation in Ohmic L-mode discharges is summarized, in III, H-mode and enhanced L-mode rotation is reviewed and in IV, the rotation in ITB plasmas is described.

II. Observed Rotation in Ohmic L-mode Plasmas

Toroidal rotation in Ohmic L-mode plasmas exhibits a rich and complex parameter dependence. The rotation velocity is found to be sensitive to the electron density, plasma current, toroidal magnetic field and magnetic configuration. It is usually

directed counter to the plasma current, with the magnitude ranging from -60 km/s (counter-current) to +20 km/s (co-current).

Shown in Fig.1 is the central toroidal rotation velocity as a function of average electron density for favorable and unfavorable ion B$\times\nabla$B drift directions in L-mode plasmas with both forward and reversed magnetic field. In L-mode plasmas the rotation is usually in the counter-current direction [23], consistent with neo-classical predictions for on-axis rotation [24]. For ∇B drift down ($\sim$lower portion of plot), there is considerable difference between LSN (favorable) and USN (unfavorable), at the higher densities ($\geq 1\times10^{20}$/m^3) for these 5.4 T, 0.8 MA discharges. This difference manifests itself in the higher H-mode power threshold [11, 12, 18, 16] for the unfavorable drift. For electron densities near 1×10^{20}/m^3, the velocities in LSN and USN are nearly the

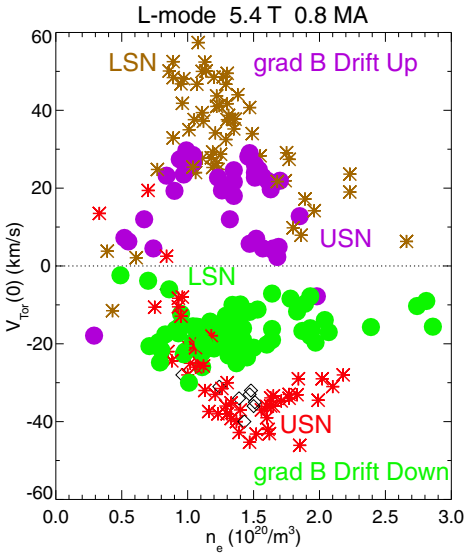

Figure 1: The ambient core rotation velocity as a function of electron density for 5.4 T, 0.8 MA L-mode discharges. Red asterisks are for USN and green dots are for LSN plasmas with the ∇B drift downward. Negative values denote counter-current rotation. Tan asterisks are for LSN and purple dots are for USN discharges with the ∇B drift upward, and with positive values for counter-current rotation. Dots are for the favorable drift direction and asterisks for unfavorable. Black diamonds are for limited plasmas.

same, and for USN plasmas, as the density falls, the velocity reverses direction to co-current. Similar and possibly related rotation inversions with density have been seen in TCV plasmas [13, 14, 15, 17]. For ∇B drift up ($\sim$upper portion of plot), there is a suggestion of symmetry for USN (favorable) and LSN (unfavorable) compared to the bottom portion of the figure; for higher densities, the rotation is more counter-current for the unfavorable drift. These trends reflect, and are a result of, the differences seen

in the scrape off layer flows [12, 16]. For different magnetic fields and plasma currents, the dependence of rotation on electron density and magnetic configuration is somewhat different [18].

The rotation in DN plasmas can be anywhere between the LSN and USN values, and depends very sensitively on SSEP, the distance between the primary and secondary separatrices [11, 12, 18]. The core rotation velocity as a function of SSEP, for different values of the electron density, is shown in Fig.2. For negative values of SSEP, which

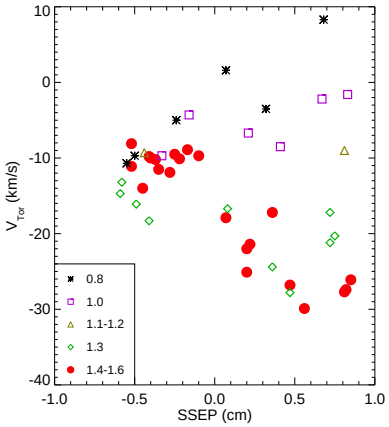

Figure 2: The central rotation velocity as a function of SSEP, sorted by average density (10^{20}/m^3), with the ∇B drift down.

is representative of LSN, there is little variation with average electron density, which is consistent with the green dots shown in Fig.1. For values of SSEP between 0.5 and 1.0 cm, which is trending towards USN, there is a strong dependence on density, similar to the red asterisks in Fig.1. For values of SSEP between -0.2 and +0.5, which corresponds to different varieties of DN plasmas, there is a concomitant intermediate dependence on electron density.

The trend of rotation direction reversal for changes in density with unfavorable drift has been observed in a single discharge by density ramping, as has been observed in TCV. Shown in Fig.3 are the time histories of the electron density and central rotation velocity for a 1.2 MA, USN discharge with a density ramp beginning at 1.1 s. Similar to the TCV results, there is an inversion of the rotation velocity from co- to counter-current as the electron density crosses a critical value (near 1.2 s), which for these conditions is around 1.6×10^{20}/m^3. The density value for the inversion during the density ramp down (at 0.6 s) was around 1.45×10^{20}/m^3, so there is some hysteresis. This may be due to a momentum confinement time longer than the particle confinement time.

Changes in plasma current or magnetic field can also lead to rotation reversal. Shown in Fig.4 is the central toroidal rotation velocity as a function of magnetic field at constant electron density for 0.8 MA LSN (favorable drift) plasmas, during a shot to

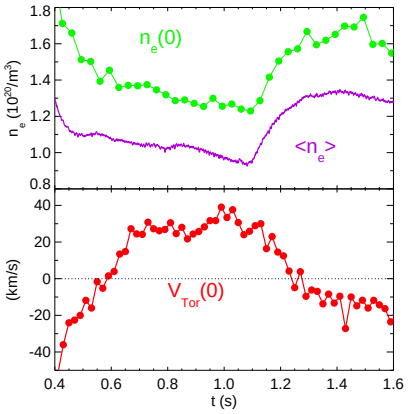

Figure 3: Time histories of the electron density (top) and the central toroidal rotation velocity (bottom) for a 1.2 MA, USN discharge with a density ramp.

shot scan. As the magnetic filed is lowered, the rotation velocity trends from strongly counter-current toward zero velocity [18]. This effect may also be achieved dynamically during a single discharge, as shown in Fig.5. As the magnetic field is ramped down from 4.5 to 3.3 T (between 0.4 and 0.8 s), the rotation velocity decreases from 30 km/s in the counter-current direction to around 0. At 0.83 s, when the velocity is close to stagnant, the plasma makes a transition to H-mode, suggesting the importance of rotation in the H-mode transition process. This is not to suggest that the *core* rotation switching from counter- to co- is the relevant condition for the H-mode transition. It is the edge rotation or velocity shear that is most important- the core rotation, which has been shown to respond to changes in the edge [12], is merely a reliable indicator. This is very similar to the situation with an ICRF power ramp in an unfavorable drift plasma, where the H-mode transition was found to occur when the rotation velocity was also near zero [18]. This is also consistent with the H-mode power threshold scaling with B_T [25, 26].

III. Observed Rotation in H-mode and Enhanced L-mode Plasmas

Core rotation in Alcator C-Mod (ICRF and Ohmic) H-mode (and enhanced confinement L-mode plasmas) without external momentum input has been found to be mostly in the co-current direction [27, 28, 29, 30, 31, 32, 33, 34]. Similar observations have been made in COMPASS-D [35] (Ohmic), JET [36] (ICRF) and DIII-D [37] (ECH and Ohmic) plasmas. An example of an ICRF heated C-Mod H-mode is shown in Fig.6. There is strong co-current rotation, with a core velocity up to 70 km/s, following the H-mode transition at 0.77s. The rotation time history follows the stored energy evolution, with a delay due to the momentum transport from the edge plasma. Co-current central

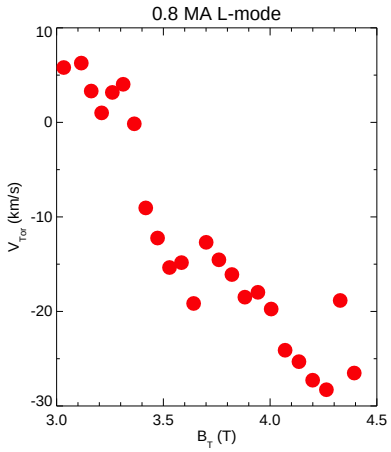

Figure 4: The central toroidal rotation velocity as a function of toroidal magnetic field for 0.8 MA, LSN L-mode discharges with an electron density of $1.0\times10^{20}/\mathrm{m}^3$.

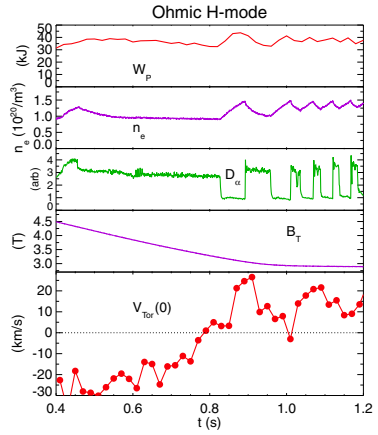

Figure 5: Time histories (from top to bottom) of the stored energy, electron density, D_α brightness, toroidal magnetic field and central rotation velocity for a 0.8 MA Ohmic H-mode plasma.

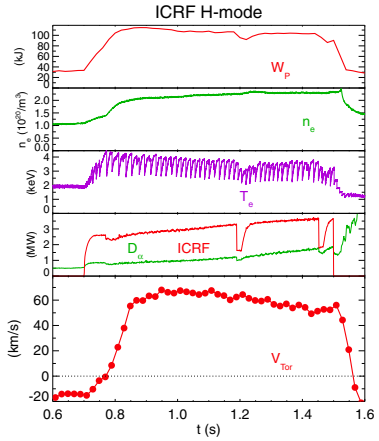

Figure 6: Time histories (from top to bottom) of the plasma stored energy, electron density, central electron temperature, ICRF power, D_α brightness and central rotation velocity for a 0.8 MA ICRF heated H-mode plasma.

rotation is indicative of a positive core radial electric field. The complete E_r profile evolution for this discharge is shown in Fig.7, which is inferred from the product of the measured toroidal rotation profile and the calculated poloidal magnetic field. For this inner region of the plasma (r/a $\leq$ 0.8), there is no evidence for any poloidal rotation and the diamagnetic contribution is small because of the large value for Z for argon [27]. Before the ICRF injection at 0.7s, the rotation is in the counter-current direction and the radial electric field is negative, with a value of around -15 kV/m near r/a=0.5. During the fully developed H-mode phase, E_r reaches a value of +40 kV/m near r/a=0.4.

A database containing nearly 1000 discharges has been populated from plasmas under a wide range of 'machine' parameters, electron density (0.6 to 6 $\times 10^{20}$/m^3), plasma current (0.4 to 1.6 MA), magnetic field (2.1 to 7.9 T) and ICRF power (0 to 5.5 MW), with forward and reverse current, in an assortment of magnetic configurations: USN, LSN, DN and inner wall limited. The best simple minded scaling with dimensional parameters for H-mode and enhanced L-mode plasmas is shown in Fig.8, which depicts the change in the central rotation velocity, between L- and (EDA and ELM-free) H-mode, as a function of the change in the stored energy, normalized to the plasma current. The red points represent a binned average of the data points and the red curve is the best linear fit, which is very close to $\Delta V_{\rm Tor}(0) = \Delta W_{\rm P}/I_{\rm P}$. This is very similar to Fig.2 of Ref.[31]. The fits as a function of $\Delta W_{\rm P}$ or $\Delta W_{\rm P}/I_{\rm P}{}^2$ are not as good, with lower correlation coefficients. The best simple minded scaling with dimensionless parameters is shown in Fig.9, which is a plot of the change in the ion thermal Mach number as a function of the change in normalized plasma pressure, β_N. This scaling has been found to capture the trends on several different devices [10].

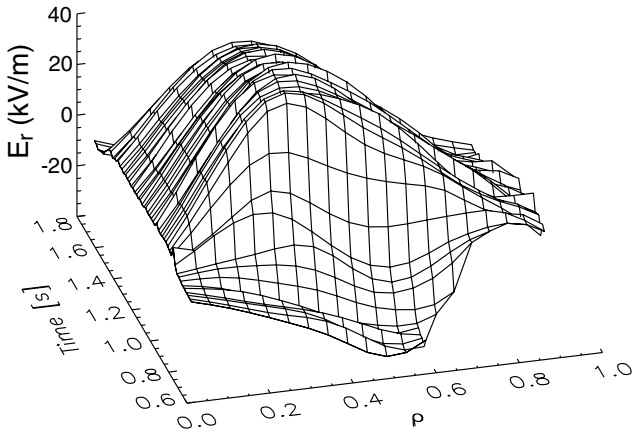

Figure 7: The inferred radial electric field profile evolution for an H-mode discharge.

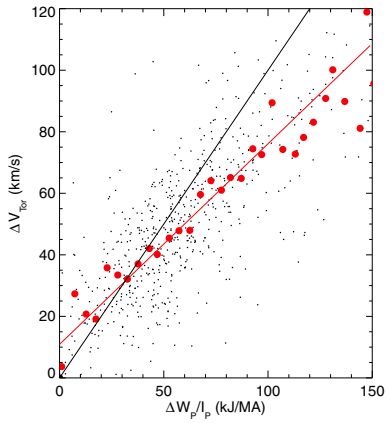

Figure 8: The change in the central toroidal rotation velocity as a function of the change in the plasma stored energy, normalized to the plasma current. The red points represent the binned average. The red curve is the best linear fit, while the black line has a slope of unity.

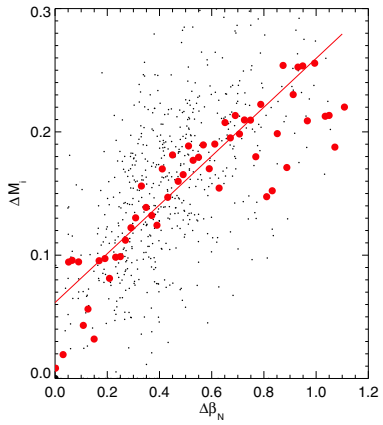

Figure 9: The change in the ion thermal Mach number as a function of the change in the normalized pressure. The red points are the binned averages, and the red line is the best fit.

IV. Rotation in ITB Plasmas

Previously, plasmas with ITBs have been produced in Alcator C-Mod with off-axis ICRF heating, and have formed naturally in certain Ohmic H-mode discharges [31, 38, 39, 40, 41, 42]. These ITBs are characterized by very peaked density profiles, which develop over a time scale considerably longer than the energy confinement time, and evolve from certain H-mode discharges. Concurrent with the density peaking is a reduction and reversal (usually) of the core (inside of the ITB foot) rotation velocity. A typical example of an off-axis ICRF heated ITB discharge is shown in Fig.10. In the middle frame is the density peaking factor, the ratio between the central electron density and that at r/a = 0.7. The usual sequence of events for ITBs induced with off-axis ICRF heating is first an L- to H-mode transition (in this case at 0.71 s), after which the electron density builds up at the edge, and then fills in to a relatively flat profile on a particle transport time scale. During this same interval, the toroidal rotation jumps to a co-current value at the edge, then propagates in to the center on a similar momentum confinement time scale [32, 33]. The H-mode is fully developed at 0.85 s in this discharge. The next sequence is the relatively slow (100s of msec, much longer than energy, particle and momentum confinement times) peaking of the electron density and a counter-current trend of the rotation velocity, which in this plasma occurs between 0.85 and 1.4 s. Remarkably similar behavior is seen in LHCD L-mode discharges [43], as seen in Fig.11. Following application of LHCD power at 0.7 s, there is a similarly slow increase in the density peaking factor and a corresponding counter-current trend in the central toroidal rotation velocity. The time scale for these events is close to the current relaxation time, but long compared to the transport times. Why the time scales for the ITB development in these two very different types of plasmas is not known.

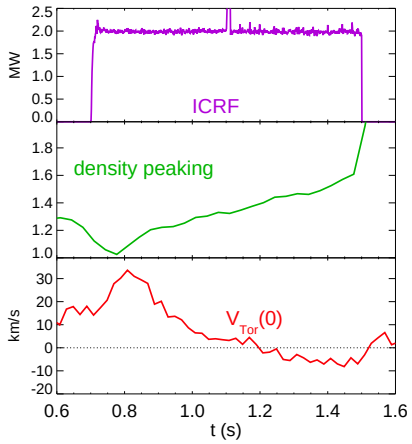

Figure 10: Time histories (from top to bottom) of the ICRF heating power, density peaking factor and central toroidal rotation velocity for an ICRF induced ITB discharge.

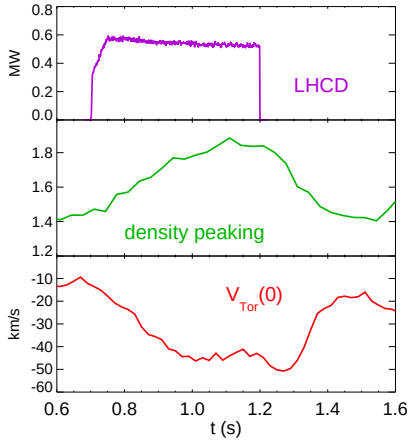

Figure 11: Time histories (from top to bottom) of the LHCD power, density peaking factor and central toroidal rotation velocity for a LHCD induced ITB discharge.

V. Discussion and Conclusions

Spontaneous rotation in C-Mod plasmas exhibits a rich phenomenology. In Ohmic L-mode discharges, the rotation is mostly in the counter-current direction, has a complex dependence on electron density, plasma current and magnetic configuration and comprises an important factor in the H-mode power threshold. A complete understanding of the H-mode transition must include the role of rotation. In H-mode and ICRF heated enhanced L-mode plasmas, the core toroidal rotation is predominantly co-current and follows a relatively simple scaling, with the rotation velocity proportional to the stored energy (pressure) normalized to the plasma current. Extrapolation of these results to ITER plasmas suggests that the expected spontaneous rotation may be large enough for RWM suppression without necessitating neutral beam injection. In ITB plasmas, the rotation inside of the barrier foot trends in the counter-current direction, and illustrates the interplay between particle, energy and momentum transport These discharges demonstrate a correlation between an inward particle pinch and an outward momentum pinch.

VI. Acknowledgements

The authors thank J. Terry for D_α measurements, J.W. Hughes for providing electron density and temperature profiles, M. Bitter for development of the imaging x-ray spectrometer, J. Irby for electron density measurements, S. Wolfe for EFIT reconstructions, A. Hubbard for electron temperature measurements, T. Abrams for assistance with the data base and the Alcator C-Mod operations, LHCD and ICRF groups for expert running of the tokamak. Work supported at MIT by DoE Contract No. DE-FC02-99ER54512.

References

[1] K.C.Shaing and E.C.Crume, Phys. Rev. Lett. **63** (1989) 2369.

[2] H.Biglari et al., Phys. Fluids **B2** (1990) 1.

[3] R.J.Groebner et al., Phys. Rev. Lett. **64** (1990) 3015.

[4] K.Ida et al., Phys. Rev. Lett. **65** (1990) 1364.

[5] P.W.Terry, Rev. Mod. Phys. **72** (2000) 109.

[6] T.S.Hahm, Phys. Plasmas **1** (1994) 2940.

[7] K.Burrell, Phys. Plasmas **4** (1997) 1499.

[8] E.J.Strait et al., Phys. Rev. Lett. **74** (1994) 2483.

[9] L.-J.Zheng et al., Phys. Rev. Lett **95** (2005) 255003.

[10] J.E.Rice et al., Nucl. Fusion **47** (2007) 1618 and references therein.

[11] J.E.Rice et al., Nucl. Fusion **44** (2004) 379.

[12] B.LaBombard et al., Nucl. Fusion **44** (2004) 1047.

[13] A.Scarabosio et al., Plasma Phys. Contr. Fusion **48** (2006) 663.

[14] A.Bortolon et al., Phys. Rev. Lett. **97** (2006) 235003.

[15] B.P.Duval et al., Plasma Phys. Contr. Fusion **49** (2007) B195.

[16] B.LaBombard et al., Phys. Plasmas **15** (2008) 056106.

[17] B.P.Duval et al., Phys. Plasmas **15** (2008) 056113.

[18] J.E.Rice et al., Nucl. Fusion **45** (2005) 251.

[19] E.S.Marmar et al., Fusion Sci. Technol. **51** (2007) 261.

[20] P.T.Bonoli et al., Fusion Sci. Technol. **51** (2007) 401.

[21] J.E.Rice et al., Rev. Sci. Instrum. **61** (1990) 2753.

[22] A.Ince-Cushman et al., "Spatially Resolved High Resolution X-ray Spectroscopy for Magnetically Confined Fusion Plasmas", submitted to Rev. Sci. Instrum. (2008).

[23] J.E.Rice et al., Nucl. Fusion **37** (1997) 421.

[24] Y.B.Kim et al., Phys. Fluids **B3** (1991) 2050.

[25] J.A.Snipes et al., Plasma Phys. Contr. Fusion **42** (2000) A299.

[26] F.Ryter et al., Plasma Phys. Contr. Fusion **44** (2002) A415.

[27] J.E.Rice et al., Nucl. Fusion **38** (1998) 75.

[28] J.E.Rice et al., Nucl. Fusion **39** (1999) 1175.

[29] I.H.Hutchinson et al., Phys. Rev. Lett. **84** (2000) 3330.

[30] J.E.Rice et al., Phys. Plasmas **7** (2000) 1825.

[31] J.E.Rice et al., Nucl. Fusion **41** (2001) 277.

[32] W.D.Lee et al., Phys. Rev. Lett. **91** (2003) 205003.

[33] J.E.Rice et al., Phys. Plasmas **11** (2004) 2427.

[34] J.E.Rice et al., Fusion Sci. Technol. **51** (2007) 288.

[35] I.H. Coffey, R. Barnsley, F.P. Keenan *et al.*, in Proceedings of the 11th Colloquium on UV and X-ray Spectroscopy of Astrophysical and Laboratory Plasmas, Nagoya, Japan, 1995, p.431, Frontiers Science Series No.15 (Editors: K. Yamashita and T. Watanabe), Universal Academy Press, Tokyo, Japan, 1996

[36] L.-G.Eriksson et al., Plasma Phys. Contr. Fusion **39** (1997) 27.

[37] J.S.deGrassie et al., Phys. Plasmas **14** (2007) 056115.

[38] C.L.Fiore et al., Phys. Plasmas **8** (2001) 2023.

[39] J.E.Rice et al., Nucl. Fusion **42** (2002) 510.

[40] S.J.Wukitch et al., Phys. Plasmas **9** (2002) 2149.

[41] J.E.Rice et al., Nucl. Fusion **43** (2003) 781.

[42] C.L.Fiore et al., Fusion Sci. Technol. **51** (2007) 303.

[43] A.Ince-Cushman et al., "Observations of Self Generated Flows in Tokamak Plasmas with Lower Hybrid Driven Current", submitted to Phys. Rev. Lett. (2008).